

Synthesis and SANS Characterization of Poly(vinyl methyl ether)-*block*-polystyrene

Takahiro Hashimoto, Hirokazu Hasegawa, Takeji Hashimoto,*
Hiroshi Katayama, Masami Kamigaito, and Mitsuo Sawamoto*

Department of Polymer Chemistry, Graduate School of Engineering, Kyoto University,
Kyoto 606-01, Japan

Masayuki Imai

Neutron Scattering Laboratory, Institute for Solid State Physics, The University of Tokyo,
Tokai, Ibaraki 319-11, Japan

Received September 16, 1996; Revised Manuscript Received September 4, 1997[®]

ABSTRACT: A solid technique to synthesize genuine diblock copolymers of poly(vinyl methyl ether) (PVME) and polystyrene (PS) for the phase behavior study was developed by the coupling reaction between end-chlorinated PVME and living PS anions. The phase behavior of the block copolymer with deuterium-labeled PS (PVME-*b*-DPS) was investigated by the small-angle neutron scattering (SANS) technique. The existence of a single broad peak in the SANS profile strongly suggested the formation of PVME-*b*-DPS block copolymer. Although the block copolymer was totally in the disordered state within the temperature range between 34 and 206 °C, an increase in the scattering intensity with temperature implying an increase in the amplitude of thermal concentration fluctuation was clearly observed, as expected from the LCST-type phase behavior of PVME/PS blends.

I. Introduction

Unlike polystyrene-*block*-polyisoprene block copolymer (PS-*b*-PI)¹ and related polymer blends that show the upper critical solution temperature (UCST)-type behavior, poly(vinyl methyl ether) and polystyrene blends (PVME/PS) are unique in that they give a phase diagram with the lower critical solution temperature (LCST).² Simply replacing the PVME component therein with poly(vinyl ethyl ether), structurally very similar to the methyl derivative but carrying the one carbon longer pendent ethyl, in turn leads to usual UCST-type phase diagrams. Perhaps PVME/PS blends are among very few examples ever known that exhibit LCST in the temperature range (ambient to 100 °C) convenient for experimental analysis. It is, therefore, not too surprising that they have been eliciting intense interest and extensive studies among polymer physicists, as witnessed in the recent abundant publications.

It is also a logical consequence to ask: What is the phase diagram of poly(vinyl methyl ether)-*block*-polystyrene block copolymer (PVME-*b*-PS), where the unique pair of the two homopolymers is connected by just a single covalent bond? This is our primary interest in PVME-*b*-PS, along with the amphiphilic properties expected for the combination of the hydrophilic/water-soluble PVME and the hydrophobic PS chains, which would in turn lead to an unprecedented phase separation phenomenon as well.

In this regard, an interesting paper has recently been published by Dudowicz and Freed,³ who theoretically predicted that PVME-*b*-PS would show both UCST and LCST-type phase behaviors⁴ to give a loop phase diagram involving a closed loop-shaped two-phase region similar to those for the water/nicotine system, poly(ϵ -caprolactone)/poly(styrene-*ran*-acrylonitrile) blends,⁵ and isotactic polypropylene/partially hydrogenated oligo(styrene-*co*-indene) blends.⁶ Besides these, loop phase

diagrams have hardly been observed experimentally, in particular, none for block copolymers.

The phase diagrams of block copolymers that exhibit both upper and lower order–disorder transition curves are classified into two types: one is a loop phase diagram that exhibits the immiscible region between the upper and lower coexistence curves; the other is a phase diagram that exhibits the miscible region between the two transition curves. The latter has been reported experimentally by Russel et al.⁷ and theoretically by Yeung et al.⁸ Despite such growing interest, however, nobody has reported thus far the experimentally observed phase diagram and the microphase separation behavior of PVME-*b*-PS, because of the technical difficulty in the synthesis of its well-defined samples.

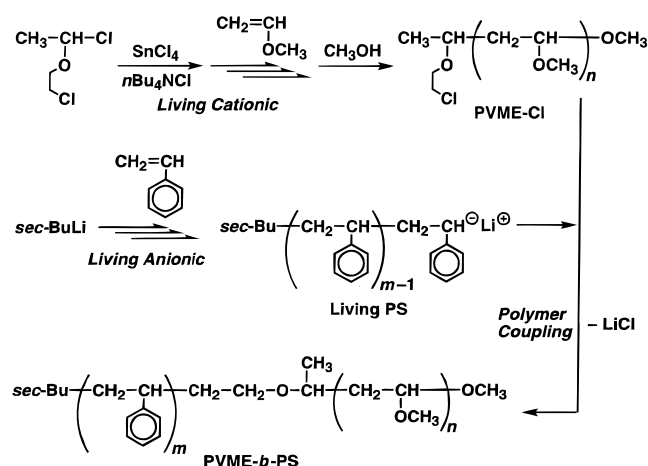
Some of us⁹ have recently synthesized PVME-*b*-PS by the sequential living cationic polymerization of the two monomers (from VME to styrene) with the hydrogen chloride/tin tetrachloride (HCl/SnCl₄) initiating system in the presence of an added salt, tetrabutylammonium chloride (*n*Bu₄NCl).¹⁰ Though it may be effective for PVME-*b*-PS of relatively short chain lengths [below 50 in number average degree of polymerization (*N*_n) for each], this method finds difficulty when we attempt to synthesize samples with block chains long enough for studying phase separation behavior. The major obstacle therein most likely appears to be the serious retardation in the second stage polymerization of styrene from the living PVME, because the pendent methyl ether moieties complex with SnCl₄ and thereby decrease its effective concentration.⁹

With phase separation analysis in mind, we herein adopted another methodology to synthesize well-defined PVME-*b*-PS with larger *N*_n. As illustrated in Scheme 1, the new methodology consists of two steps, the synthesis of an end-chlorinated poly(vinyl methyl ether) (PVME-Cl) carrying a primary alkyl chloride terminal, followed by its coupling reaction with living anionic polystyrene. PVME-Cl was obtained by the living cationic polymerization of VME initiated with the hydrogen chloride adduct of 2-chloroethyl vinyl ether

* To whom correspondence should be addressed.

[®] Abstract published in *Advance ACS Abstracts*, October 1, 1997.

Scheme 1. Synthesis of PVME-*b*-PS by Coupling Reaction



(HCl-CEVE), which is regarded as a functionalized initiator with a 2-chloroethyl group that can effectively quench polystyryl carbanions. The HCl-CEVE initiator was combined with SnCl₄ as a Lewis acid-type activator in conjunction with an added *n*Bu₄NCl salt in dichloromethane (CH₂Cl₂) solvent at -78 °C. Because this system induces living polymerization of VME,⁹ as demonstrated in this work as well, the resulting polymer has a terminal chloroethyl group derived from the initiator, in addition to a controlled molecular weight and a very narrow molecular weight distribution (MWD). The living polystyryl anions were prepared by the conventional living anionic polymerization of styrene with *sec*-butyllithium (*s*BuLi).

Another possible route for preparation of PVME-*b*-PS would of course be direct in-situ coupling between a living cationic PVME and a living anionic PS,¹¹ but we decided not to employ it, because our preliminary attempts soon revealed that CH₂Cl₂, the solvent of choice for the living VME polymerization,⁹ obviously undergoes undesired quenching of the carbanion by itself.

In this paper, we report the synthesis of well-defined PVME-*b*-PS samples via the coupling reaction of a PVME-Cl with a living PS (Scheme 1), its extension to the preparation of the deuterated versions (PVME-*b*-DPS) with styrene-*d*₈, and the first analysis of the phase behavior of PVME-*b*-DPS by the small-angle neutron scattering (SANS) technique. PVME-*b*-DPS was designed to examine the loop phase diagram predicted by Dudowicz and Freed³ and synthesized to have the degree of polymerization $N_n = 3.3 \times 10^2$ and the fraction of DPS $f_{\text{DPS}} = 0.27$. According to the prediction by Dudowicz and Freed, the order-disorder transition should occur at ca. 30 and 180 °C for the block copolymer with such molecular weight and composition. The microphase separation should occur between these temperatures.

The experimental studies of the phase behavior of PVME-*b*-PS have been far behind the theoretical studies because of the technical difficulty in the synthesis of PVME-*b*-PS. We believe that our work is really the first one to show the solid technique to synthesize genuine PVME-*b*-PS and to characterize the phase behavior experimentally.

II. Experimental Section

Materials. Vinyl methyl ether (Tokyo Kasei; purity >99%), commercially obtained in a small gas cylinder, was condensed

under dry nitrogen at -78 °C just before use into a baked graduated glass tube equipped with a three-way stopcock, where the liquefied monomer was diluted with CH₂Cl₂ into a stock monomer solution at a known concentration. 2-Chloroethyl vinyl ether (Nisso Maruzen Chemical; purity >99.5%), styrene (Wako Chemicals; purity >98%), α -methylstyrene (α MS; Wako Chemicals; purity >98%), and deuterated styrene (styrene-*d*₈) were washed with aqueous 10% sodium hydroxide solution and then with water, dried overnight with anhydrous sodium sulfate, and distilled twice over calcium hydride under atmospheric pressure (CEVE), reduced pressure (styrene and α -methylstyrene), or high vacuum (deuterated styrene). Solutions of SnCl₄ (1.0 M in CH₂Cl₂) and *s*BuLi (1.0 M in cyclohexane), both from Aldrich, were used as received. Commercial *n*Bu₄NCl (Tokyo Kasei; purity >99%) was used as supplied after drying under vacuum at room temperature. The initiator (HCl-CEVE) was prepared by electrophilic addition of hydrogen chloride to CEVE in *n*-hexane, as reported previously.^{12,13} CH₂Cl₂ was dried overnight over calcium chloride and distilled over phosphorus pentoxide and then over calcium hydride before use. Toluene, cyclohexane, and *n*-hexane (all guaranteed reagents, Wako Chemicals) were dried overnight over calcium chloride and distilled twice over calcium hydride before use.

Polymerization Procedures. The living polymerizations of VME and styrene and the coupling reaction were carried out under dry nitrogen in a baked glass tube equipped with a three-way stopcock and a magnetic stirring bar. All reagents were transferred via dried syringes through a three-way stopcock against a dry nitrogen stream.

A typical example of the living cationic polymerization of VME was as follows: to a cooled VME solution (1.0 M, 4.0 mL) in CH₂Cl₂ at -78 °C with vigorous stirring were added a solution of the initiator HCl-CEVE (200 mM, 0.50 mL; in *n*-hexane) and then a solution of SnCl₄ and *n*Bu₄NCl (100 mM each, 5.0 mL; in CH₂Cl₂). The polymerization mixture was thus 0.50 mL in volume where [VME]₀ = 0.80 M; [HCl-CEVE]₀ = 20 mM; [SnCl₄]₀ = [*n*Bu₄NCl]₀ = 10 mM. The reaction was quenched with prechilled ammoniacal methanol (2.0 mL). The monomer conversion was determined by gravimetry. The quenched reaction solution was diluted with toluene and washed sequentially with diluted hydrochloric acid, an aqueous sodium hydroxide solution, and water to remove the tin-containing residues, where the washing solutions were used above 40 °C to avoid loss of PVME. The organic layer was evaporated to dryness under reduced pressure and dried in vacuo overnight to give the product polymers. Apart from aliquots for analysis, the PVME-Cl samples for the coupling reaction were dissolved in 1,4-dioxane and freeze-dried.

A typical example of the living anionic polymerization of styrene was as follows:¹¹ under dry nitrogen via the syringe technique, a solution of *s*BuLi (1.0 M, 0.12 mL; in cyclohexane) was added to a solution of α MS (62.5 mM, 4.8 mL) in toluene at 30 °C to give a red solution of the α -methylstyryl anion. Styrene (5.0 M, 1.2 mL; in toluene) was added to this to give an orange solution typical for the polystyryl anion, 6.0 mL in volume, where [styrene]₀ = 1.0 M; [α MS]₀ = 50 mM; [*s*BuLi]₀ = 20 mM. The polymerization was run for 60 min, when the orange solution turned red, indicative of the growing end transformed into the α -methylstyryl anion. For the coupling reaction, a toluene solution of PVME-Cl (see above) was added to the living PS thus prepared. The mixture immediately turned colorless and was stirred for an additional 2 min. The solution was diluted with toluene and washed with water, evaporated to dryness under reduced pressure, and dried in vacuo overnight to give product polymers.

A part of the living PS solution (1.0 mL) was separately quenched with prechilled methanol (1.0 mM), and the homopolymer was recovered for the MWD analysis by the same method as that for the product polymers.

The living anionic polymerizations of deuterated styrene and the subsequent coupling reactions were carried out similarly but under high vacuum (<10⁻⁵ Torr); α MS was not employed in the initial living polymerization. The quenched solutions were diluted with cyclohexane and washed with water to

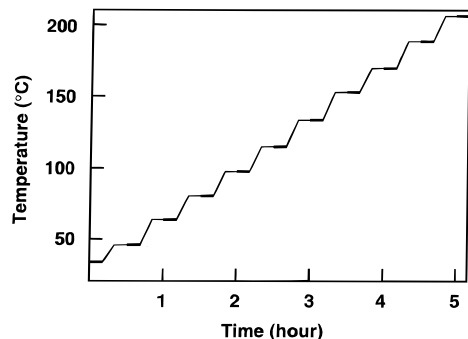


Figure 1. Thermal program used in the heating process of the SANS experiment for PVME-*b*-DPS. The thick lines indicate the period of the SANS measurement at each temperature.

remove initiator residues to give the product polymers that were further purified by freeze-drying.

Characterization of Samples. The MWD of polymers was measured by size-exclusion chromatography (SEC) in chloroform on three polystyrene gel columns (Shodex K-802, K-803, and K-804) that were connected in series to a JASCO 880-PU precision pump and a JASCO 830-RI refractive index detector. The number-average molecular weight M_n and polydispersity index M_w/M_n values of the polymers were calculated from SEC eluograms on the basis of a polystyrene calibration. Polymers used for ^1H NMR and SANS analyses were fractionated by preparative SEC (column: Shodex H-2003). ^1H NMR spectra (270 MHz) were recorded at 30 °C in deuterated chloroform on a JEOL GSX-270 spectrometer.

SANS. The sample for SANS experiments was prepared by casting 5 wt % toluene solution and evaporating the solvent under vacuum at 100 °C. The small-angle neutron scattering (SANS) experiments were carried out on the SANS-U instrument of the Institute for Solid State Physics of the University of Tokyo at the JRR-3M research reactor in Tokai. The cold neutrons were monochromatized with a velocity selector to have the mean wavelength λ of 7.0 Å with a distribution $\Delta\lambda$ ($=0.7$ Å) characterized by the full width at the half-maximum. The scattered neutrons were detected by a two-dimensional detector. The two-dimensional data were circularly averaged to obtain scattering profiles as a function of magnitude of the scattering vector q [$= (4\pi/\lambda) \sin(\theta/2)$, where θ is the scattering angle]. The scattering intensity data were corrected for empty cell scattering and sample transmission. The coherent scattering was obtained by subtracting the incoherent scattering evaluated from the high- q data of the separate measurement. But they were not reduced to absolute intensity. Figure 1 presents the temperature program for the data collection on PVME-*b*-DPS. All measurements were started about 10 min after the preset temperatures were attained.

III. Results and Discussion

Synthesis of End-Chlorinated PVME (PVME-Cl) by Living Cationic Polymerization. PVME-Cl was synthesized according to the route shown in the first part of Scheme 1. Thus, the polymerization of VME was initiated with the HCl-CEVE/ SnCl_4 system in the presence of $n\text{Bu}_4\text{NCl}$ in CH_2Cl_2 at -78 °C ($[\text{VME}]_0/[\text{HCl-CEVE}]_0/[\text{SnCl}_4]_0/[n\text{Bu}_4\text{NCl}]_0 = 800/20/10/10$ mM).⁹ The polymerization occurred smoothly without an induction phase, reaching 90% conversion in 60 min. Figure 2 shows the size-exclusion chromatograms of the PVME obtained at varying conversions. As the polymerization proceeded, the SEC eluograms shifted to higher molecular weight, while keeping unimodal and narrow MWD ($M_w/M_n < 1.1$). These results suggest that the HCl-CEVE-based system led to the living polymerization of VME.

Figure 3 gives the ^1H NMR spectrum for a typical sample of PVME thus obtained. In addition to the

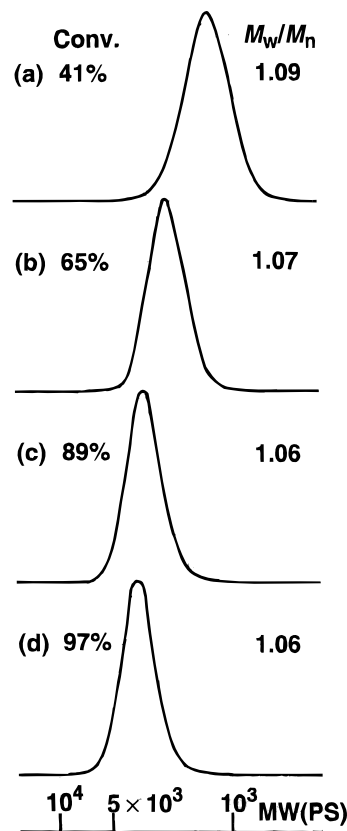


Figure 2. SEC curves of the PVME obtained at conversion (a) 41%, (b) 65%, (c) 89%, and (d) 97% in the polymerization with HCl-CEVE/ SnCl_4 in the presence of $n\text{Bu}_4\text{NCl}$ in CH_2Cl_2 at -78 °C ($[\text{VME}]_0 = 0.80$ M; $[\text{HCl-CEVE}]_0 = 20$ mM; $[\text{SnCl}_4]_0 = [n\text{Bu}_4\text{NCl}]_0 = 10$ mM). The polydispersity indices (M_w/M_n) are indicated in the figure.

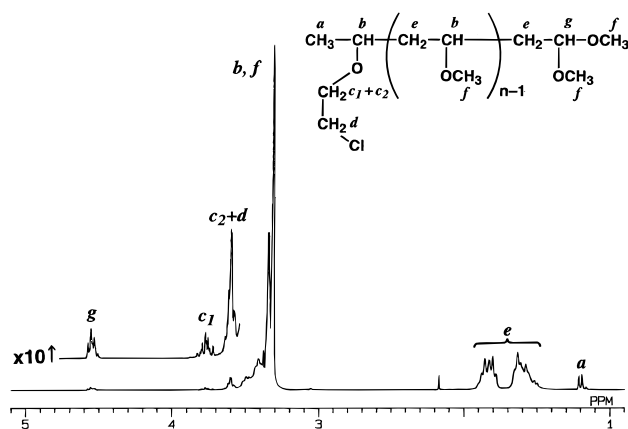


Figure 3. The ^1H NMR spectrum of PVME-Cl; the sample shown in Figure 2c. The absorption bands are assigned to the particular protons indicated in the insertion by letters a–g.

strong adsorptions (b, e, and f) of the VME units in the main chain, the spectrum exhibits characteristic signals of the terminal groups: the methyl proton (a) at the α -end and the acetal methine proton (g) at the ω -end originated from the quenching with methanol.^{9,12} The signals of the chloroethyl unit (protons c₁, c₂, and d) originated from the initiator are observed between 3.5 and 3.8 ppm. The two methylene protons (c₁ and c₂) adjacent to the ether oxygen are not spectroscopically equivalent due to the neighboring chiral methine carbon (b) and their signals are split into two. The signal c₂ overlapped the other methylene protons (d) adjacent to the pendent chlorine and was on the shoulder of the main-chain methoxy protons. These features quanti-

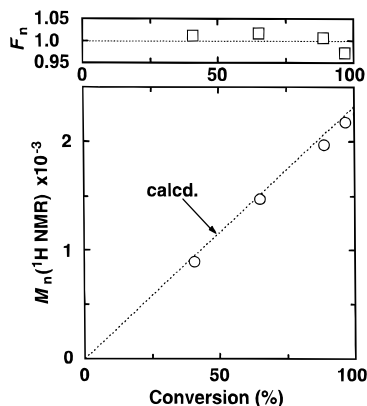


Figure 4. Plots of F_n and $M_n(^1\text{H NMR})$ of PVME obtained in the same experiments as Figure 2 as a function of conversion.

tatively verify the attachment of the CEVE initiator residue to the PVME main chain.

The number-average end-functionality (F_n) of the chloroethyl unit was determined from the peak intensity ratio (c_1/g) of one of the α -terminal methylene protons (c_1) to the ω -terminal methine proton (g). The F_n value for this particular sample was close to unity ($F_n = 1.01$), which indicates that one polymer chain carries nearly one chloroethyl unit at the α -end.

N_n was also determined from the peak intensity ratio ($e/2g$) of the main-chain methylene proton (e) to the terminal methine (g) ($N_n = 31.5$). The number-average molecular weight [$M_n(^1\text{H NMR})$] was then calculated according to eq 1, where 58.08 and 138.5 denote,

$$M_n(^1\text{H NMR}) = 58.08N_n + 138.5 \quad (1)$$

respectively, the formula weights of the VME unit and the α - and ω -terminal groups [$\text{CH}_3\text{CH}(\text{OCH}_2\text{CH}_2\text{Cl})$ - and $-\text{OCH}_3$]. The $M_n(^1\text{H NMR})$ values were also calculated for all the samples shown in Figure 2 and were plotted against conversion in Figure 4. The $M_n(^1\text{H NMR})$ values were directly proportional to monomer conversion and in good agreement with the values calculated on the assumption that one initiator molecule generates one living polymer chain (dotted line). In addition, the value of F_n was close to unity throughout the reaction. These results show the occurrence of the living polymerization of VME to give PVME-Cl.

As already reported,⁹ $M_n(^1\text{H NMR})$ for PVME is linearly correlated with M_n by SEC based on a PS calibration, and this empirical correlation was employed to determine M_n for PVME of higher molecular weight.

Synthesis of PVME-*b*-PS by Coupling Reaction. The feasibility of the coupling reaction between a PVME-Cl thus obtained and a nondeuterated living PS (Scheme 1) was then examined. The N_n of both precursors were set relatively small (~ 50 each) for the analyses. The living PS sample was separately obtained as mentioned in the Experimental Section. The M_n values of the PS samples prepared in this way were close to the calculated values, assuming that one initiator molecule generates one living PS.

Parts a and b of Figure 5, respectively, show the SEC traces for the PVME-Cl and PS samples employed, both with very narrow MWDs ($M_w/M_n = 1.05$ – 1.06). According to the $^1\text{H NMR}$ and SEC analysis, the N_n of these samples are 35 for the PVME-Cl and 52 for the PS.

The coupling reaction was performed in toluene at 30 °C, when 1.2 mol of the PVME-Cl was added into 1.0

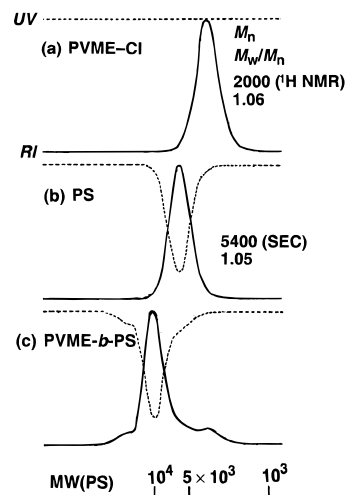


Figure 5. SEC curves of (a) PVME-Cl, (b) PS, and (c) PVME-*b*-PS obtained with a RI detector (—) and a UV detector (---) at 256 nm. PS was polymerized with *s*BuLi in the presence of a small amount of α MS in toluene at 30 °C: $[\text{styrene}]_0 = 1.0$ M; $[\text{sBuLi}]_0 = 20$ mM; $[\alpha\text{MS}]_0 = 50$ mM. PVME-*b*-PS was obtained in toluene at 30 °C by the coupling reaction between $[\text{PVME-Cl}]_0 = 11$ mM and $[\text{living PS}]_0 = 9$ mM. PVME-*b*-PS shown in the figure is as prepared and before fractionation.

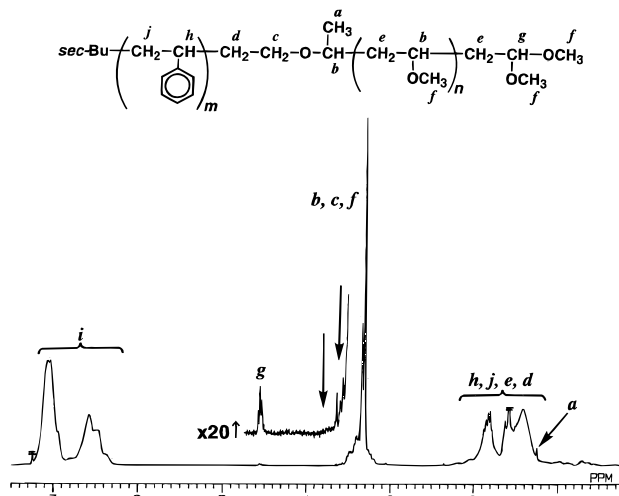


Figure 6. $^1\text{H NMR}$ spectrum of PVME-*b*-PS fractionated by preparative SEC from the sample shown in Figure 5c. The absorption bands are assigned to the particular protons indicated in the insertion by letters a–h.

mol of the living PS. In the MWD curve for the product (Figure 5c), a new fraction with the peak molecular weight almost equal to the sum of the two prepolymers emerged. This fraction had UV absorption characteristic to the PS segments. These results suggest that the living PS effectively reacted with the PVME-Cl to produce PVME-*b*-PS copolymer. The minor fractions of lower molecular weights are most likely attributed to the deactivated PS and/or PVME.

The main fraction of this sample was then separated by preparative SEC for the $^1\text{H NMR}$ structural analysis (Figure 6). The spectrum exhibits the representative signals of both VME and styrene units, for example, the methoxy proton of PVME at about 3.3 ppm and the phenyl proton of PS at about 7 ppm. Besides these strong absorptions, the ω -terminal methine proton originated from the PVME segments can be seen at 4.6 ppm, and more importantly, the methylene proton (c_1) of the terminal chloroethyl unit (3.8 ppm in Figure 3) disappeared.¹⁴ These results indicate that the chloro-

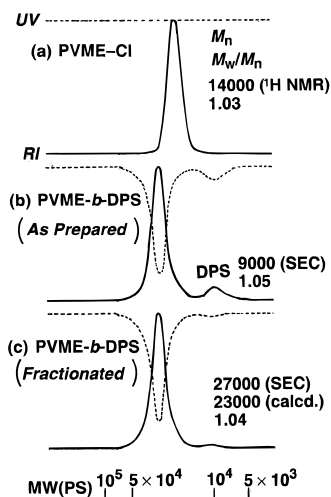


Figure 7. SEC curves of (a) PVME-Cl, (b) PVME-*b*-DPS (as prepared), and (c) PVME-*b*-DPS (fractionated) obtained with a RI detector (—) and a UV detector (---) at 256 nm. DPS was polymerized with *s*BuLi in cyclohexane at 50 °C: [styrene-*d*₈]₀ = 0.17 M; [*s*BuLi]₀ = 1.5 mM. PVME-*b*-DPS was obtained in cyclohexane at room temperature by the coupling reaction between [PVME-Cl]₀ = 0.7 mM and [living DPS]₀ = 0.8 mM.

ethyl unit in the PVME-Cl reacted with the living PS anion (more exactly, the terminal α -methylstyryl anion^{11,14}) to give the polymer with the cumyl ethyl unit. The absorption of these methylene protons probably appears at a higher magnetic field region than the chloroethyl absorption and now overlaps with the strong signals of the main-chain methoxy proton. Thus, the coupling reaction of a PVME-Cl with a living PS anion was proved to be effective in synthesizing a PVME-*b*-PS copolymer. 1H NMR and SEC analyses of the sample shown in Figure 5c gave the following results (after SEC fractionation): $N_n(^1H$ NMR) of the PVME and PS block chains are 40 and 73, respectively (35 and 52 calculated values); $M_n(SEC) = 1.2 \times 10^4$; $M_w/M_n(SEC) = 1.06$. Although the block chain lengths are probably not large enough in the feasibility study of the synthesis described above, we decided to proceed to the synthesis of PVME-*b*-DPS for SANS analysis by the same strategy.

Synthesis of PVME-*b*-DPS. Following the feasibility study, the deuterated sample PVME-*b*-DPS was synthesized in a similar way. For better reaction control, however, the *s*BuLi-initiated living anionic polymerization of styrene-*d*₈ was carried out under high vacuum in cyclohexane without using additional α MS feed. Figure 7 summarizes the results.

For the synthesis of PVME-*b*-DPS, PVME-Cl with a very narrow MWD ($M_w/M_n = 1.03$) and a higher molecular weight [$M_n(^1H$ NMR) = 1.4×10^4 or $N_n = 2.4 \times 10^2$], as shown in Figure 7a, was prepared in the same way as already discussed. A solution of this PVME-Cl was added to the living anions of styrene-*d*₈ polymer (DPS), which also had a very narrow MWD ($M_w/M_n = 1.03$) and controlled molecular weight ($M_n = 9.0 \times 10^3$ or $N_n = 90$). The coupling reaction proceeded smoothly to give a polymer with a narrow MWD, and its molecular weight clearly increased to reach over 2.0×10^4 , as expected for the coupling product (Figure 7b). A trace of the unreacted DPS is still observed, probably due to a difference in the end-group concentration between the two precursors. The SEC fractionation of the major peak led to the MWD trace shown in Figure 7c, indicating the formation of PVME-*b*-DPS with a narrow

Table 1. Characteristics of Samples Used in This Work

sample	M_n	M_w/M_n	f_{DPS}^a
PVME- <i>b</i> -DPS	23 000	1.04	0.27

^a f_{DPS} : volume fraction of DPS.

MWD. Table 1 shows the characterization data for this sample; 1H NMR analysis verified complete coupling of the two precursors through the chloroethyl terminal, which was not seen spectroscopically in the final product.

The PVME-*b*-DPS sample is especially important for the investigation of the phase behavior by a scattering technique. The contrast factor of PVME-*b*-PS for X-ray analysis given by the square of the difference between the electron densities of the two components is very small and about $1/30$ th of that of PS-*b*-PI, for which extensive studies of the order-disorder transition by small-angle X-ray scattering (SAXS) have been reported.¹ Therefore, the SAXS study of PVME-*b*-PS is almost hopeless unless a superstrong X-ray source such as synchrotron orbital radiation (SOR) is used. In fact, no appreciable scattering was observed for PVME-*b*-PS either with our X-ray source (an 18 kW rotating anode X-ray generator) or with a SOR source (BL15A, 10^3 times more powerful than ours) at the National Laboratory for High Energy Physics (KEK) in Tsukuba, Japan. On the other hand, the contrast factor for neutron scattering is given by the square of the difference between the scattering length densities of the two components. The contrast factors of PVME-*b*-PS and PS-*b*-PI for neutrons are comparable in contrast to those for X-ray. The deuteration of the polystyrene component increases the contrast factors by 29 times for PVME-*b*-PS and by 25 times for PS-*b*-PI. Since it is known that even PS-*b*-PI gives enough contrast in SANS,¹⁵ the study of PVME-*b*-DPS by SANS is certainly feasible.

The theoretical prediction of the phase behavior has been done by Dudowicz and Freed.³ Our block copolymer, PVME-*b*-DPS, was designed to test their prediction. According to their prediction (see Figure 9 of ref 3), PVME-*b*-DPS [the total degree of polymerization $N = N_{DPS} + N_{PVME} = 3.3 \times 10^2$ and the fraction of DPS $f_{DPS} = N_{DPS}/(N_{DPS} + N_{PVME}) = 0.27$] is expected to be in the disordered state at temperatures below ca. 30 °C, in the ordered state (microphase separated) between ca. 30 and ca. 180 °C, and again in the disordered state above ca. 180 °C. Thus, we might be able to observe both transitions, the LCST-type order-disorder transition at ca. 30 °C and the UCST-type order-disorder transition at ca. 180 °C, or at least one of them in the course of the heating experiment from 34 to 206 °C, which may be the upper limit of temperature attainable without significant degradation of the sample copolymer.

SANS Measurement of PVME-*b*-DPS. Figure 8 illustrates the SANS profiles for PVME-*b*-DPS at various temperatures (following the thermal program shown in Figure 1). The scattering intensity in arbitrary units (au) is plotted against the magnitude of the scattering vector q in a linear scale. The scattering intensity was extremely weak but increased with rising temperature. The SANS profiles exhibit a broad single peak at about $q = 3.9 \times 10^{-2} \text{ \AA}^{-1}$ and no higher-order peak was observed in the temperature range of our investigation although the entire scattering profiles are not shown in Figure 8. The existence of the scattering peak is a good indication of the existence of a block copolymer in

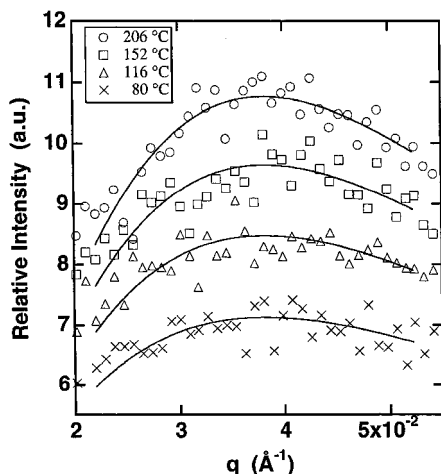


Figure 8. Temperature dependence of the SANS profiles for PVME-*b*-DPS shown in Table 1. The solid lines are the best-fitted theoretical curves with eq 2.

either the ordered or disordered state. In the ordered state, the periodic concentration fluctuation due to the microdomain structure causes one or more scattering peaks¹⁶ while a single scattering peak due to the correlation hole is usually observed in the disordered state.¹ A scattering peak may be observed for a polymer blend undergoing spinodal decomposition even in the absence of a block copolymer. It could have happened if the coupling reaction between the living PS and the PVME-Cl was unsuccessful. But this possibility can be excluded because the scattering peak should grow in intensity and shift toward smaller q with time in such a case.¹⁷ The peak position of the scattering profiles in Figure 8 hardly shifts with temperature or with time. This evidence together with the SEC and ¹H NMR results is sufficient proof of success in our synthesis of PVME-*b*-PS.

The SANS scattering peak of PVME-*b*-DPS is broad and weak in intensity, and becomes insignificant at the temperatures below ca. 80 °C. This strongly suggests that the copolymer is in the disordered state at all temperatures (34–206 °C) investigated in this study. According to the simple mean-field theory,¹⁸ block copolymers have a greater tendency to mix than the blends of the corresponding homopolymers. A DPS/PVME blend similar in composition to the PVME-*b*-DPS block copolymer but having much higher molecular weights (7–28 times higher) was reported to exhibit its LCST at ca. 150 °C.¹⁹ Therefore, the order–disorder transition temperature of PVME-*b*-DPS is expected to be much higher than the upper limit of our experiment (206 °C). Consequently, PVME-*b*-DPS in the temperature range of our SANS measurement must be in the deep disordered state according to the simple mean-field theory. This is in good agreement with our observation. At this moment we would rather think that the prediction by Freed et al. in the context of the lattice cluster theory gave a surprising result.

For the disordered state of a diblock copolymer, Leibler's mean-field theory¹⁸ predicts that $I(q)$ at q is given by eq 2, where χ is the Flory–Huggins segmental

$$I(q) \sim N/[F(q) - 2\chi N] \quad (2)$$

interaction parameter and $F(q)$ is a function that depends on the composition (f) and the gyration radius (R_g) of the block copolymer. In the case of a pure diblock copolymer, $F(q)$ is a function having a minimum, and

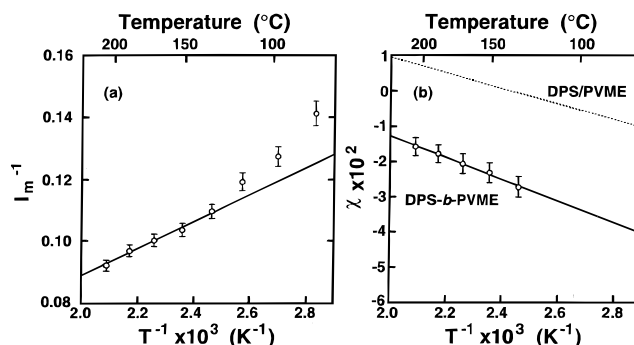


Figure 9. (a) I_m^{-1} vs T^{-1} and (b) χ vs T^{-1} for PVME-*b*-DPS. The solid line ($\chi = 0.048 - 31 T^{-1}$) is obtained by the least-squares fit to the four data points at higher temperatures. The dotted line ($\chi = 0.053 - 22 T^{-1}$) shows the temperature dependence of χ for PVME/DPS.¹⁹

hence $I(q)$ is a function having a maximum. We denote the maximum value of $I(q)$ by I_m and the corresponding q by q_m . The value of q_m does not explicitly depend on χ and hence on temperature. If χ is a function of temperature T given by

$$\chi = A + BT^{-1} \quad (3)$$

I_m^{-1} should change linearly with T^{-1} in the disordered state in the mean-field regime whereas the characteristic length ($D \equiv 2\pi/q_m$) of the thermal concentration fluctuation remains constant with T^{-1} .

Assuming that our system is in the disordered state in the mean-field regime over the temperature range covered, the SANS data in Figure 8 were analyzed by fitting theoretical scattering curves calculated with eq 2. The best-fitted curves are shown by the solid curves in Figure 8. The values of I_m^{-1} and χ were obtained as the fitting parameters. Figure 9a shows the plot of I_m^{-1} vs T^{-1} . In the higher temperature range ($T^{-1} < 2.4 \times 10^{-3} \text{ K}^{-1}$), I_m^{-1} is reasonably linear with T^{-1} , suggesting that PVME-*b*-DPS is in the disordered state and in the mean-field regime. I_m^{-1} deviates from the line at the lower temperatures. It is probably due to the lower signal-to-noise ratio at those temperatures. Therefore, the value of χ estimated for PVME-*b*-DPS was plotted only for the higher temperatures in Figure 9b. It should be noted that the value of χ is negative in the experimental temperature range, indicating the attractive interaction between PVME and DPS chains. The tendency of I_m and χ increasing with T suggests an increase in the segregation power with T . This is characteristic of the LCST-type phase behavior that was expected from the behavior of PVME/PS blends.² The temperature dependence of χ for PVME-*b*-DPS estimated from the linear region of the χ vs T^{-1} plot χ_{block} is given by

$$\chi_{\text{block}} = 0.048 - 31 T^{-1} \quad (4)$$

The mean-field spinodal temperature (T_s) can be estimated by extrapolating the linear relation between I_m^{-1} and T^{-1} (as shown in Figure 9a) to the T^{-1} value at which I_m^{-1} goes to zero on the basis of eqs 2 and 3. However, T_s^{-1} thus estimated becomes negative. This might imply that the slope of the fitted line in Figure 9a is somewhat smaller than what we normally expect. If we take into account the systematic deviation of the data points for lower temperatures from the linear relationship, the temperature dependence of I_m seems to parallel the prediction by Dudowicz and Freed,³ in

which I_m should increase first and then decrease with T . Therefore, further investigation is necessary, but it is beyond the scope of this work.

The temperature dependence of χ for a PVME/DPS blend (χ_{blend}) with the similar composition evaluated from Figure 10 in ref 19 is written as

$$\chi_{\text{blend}} = 0.053 - 22 T^{-1} \quad (5)$$

and the result was plotted with the dotted line in Figure 9b. Comparing eqs 4 and 5, the values of χ_{block} are much smaller than those of χ_{blend} over the temperature range covered in this experiment. This implies that the connectivity between PS and PVME blocks is very important. Our preliminary result shows that the connectivity appears to affect both A and B in eq 3. But detailed investigation such as composition and molecular-weight dependencies of χ_{block} deserves future work and publication, and is beyond the scope of this work.

IV. Conclusion

The end-chlorinated PVME (PVME-Cl) was synthesized by the living cationic polymerization of VME with the HCl-CEVE/SnCl₄ system in the presence of *n*Bu₄NCl in CH₂Cl₂ at -78°C . PVME-*b*-PS was successfully synthesized by the coupling reaction between PVME-Cl and the living PS anion.

The SANS profiles with a single scattering peak, implying that the block copolymer was in the disordered state, were observed at all temperatures investigated (34–206 °C) for PVME-*b*-DPS with $M_n = 2.3 \times 10^4$, $M_w/M_n = 1.04$, and $f_{\text{DPS}} = 0.27$. Namely, the copolymer was totally in the disordered state. An increase in the scattering intensity with increasing temperature between 34 and 206 °C suggests the LCST-type phase behavior of PVME-*b*-DPS; i.e., the segregation power increases with increasing temperature. Moreover, the phase transition expected for the loop phase diagram predicted by Dudowicz and Freed³ was not observed.

Acknowledgment. This work was supported in part by a Grant-in-Aid for Scientific Research in Priority Areas "New Polymers and Their Nano Organized Systems" from the Ministry of Education, Science, Sports, and Culture, Japan.

References and Notes

- (1) Mori, K.; Hasegawa, K.; Hashimoto, T. *Polym. J.* **1985**, *17*, 799. Hashimoto, T.; Ijichi, Y.; Fetters, L. J. *J. Chem. Phys.* **1988**, *89*, 2463. Hashimoto, T.; Ogawa, T.; Han, C. D. *J. Phys. Soc. Jpn.* **1994**, *63*, 2206. Sakamoto, N.; Hashimoto, T. *Macromolecules* **1995**, *28*, 6825. Mori, K.; Okawara, A.; Hashimoto, T. *J. Chem. Phys.* **1996**, *104*, 7765.
- (2) Kwei, T. K.; Nishi, T.; Roberts, R. F. *Macromolecules* **1974**, *7*, 667. Nishi, T.; Wang, T. T.; Kwei, T. K. *Macromolecules* **1975**, *8*, 227. Nishi, T.; Kwei, T. K. *Polymer* **1975**, *16*, 285.
- (3) Dudowicz, J.; Freed, K. F. *Macromolecules* **1993**, *26*, 213.
- (4) In this paper we use the expression "LCST-type (or UCST-type) phase behavior" in the case of an increase (or decrease) in the segregation power with increasing temperature.
- (5) Svoboda, P.; Kressler, J.; Chiba, T.; Inoue, T.; Kammer, H. W. *Macromolecules* **1994**, *27*, 1154.
- (6) Lee, C. H.; Saito, H.; Goizueta, G.; Inoue, T. *Macromolecules* **1996**, *29*, 4274.
- (7) Russell, T. P.; Karis, T. E.; Gallot, Y.; Mayes, A. M. *Nature* **1994**, *368*, 729. Karis, T. E.; Russell, T. P.; Gallot, Y.; Mayes, A. M. *Macromolecules* **1995**, *28*, 1129.
- (8) Yeung, C.; Desai, R. C.; Shi, A.-C.; Noolandi, J. *Phys. Rev. Lett.* **1994**, *72*, 1834.
- (9) Ohmura, T.; Sawamoto, M.; Higashimura, T. *Macromolecules* **1994**, *27*, 3714.
- (10) Ishihama, Y.; Sawamoto, M.; Higashimura, T. *Polym. Bull.* **1990**, *24*, 201. Higashimura, T.; Ishihama, Y.; Sawamoto, M. *Macromolecules* **1993**, *26*, 744.
- (11) Creutz, S.; Vandooren, C.; Jerome, R.; Teyssie, P. *Polym. Bull.* **1994**, *33*, 21.
- (12) Katayama, H.; Kamigaito, M.; Sawamoto, M.; Higashimura, T. *Macromolecules* **1995**, *28*, 3747.
- (13) Higashimura, T.; Kamigaito, M.; Kato, M.; Hasebe, T.; Sawamoto, M. *Macromolecules* **1993**, *26*, 2670.
- (14) Some weak signals seen at 0.5–1 ppm are due to the very short α MS units attached to the starting PS sample. The use of a small amount of α MS was needed to control the living anionic polymerization of styrene under dry nitrogen.⁹
- (15) Hasegawa, H.; Hashimoto, T.; Kawai, H.; Lodge, T. P.; Amis, E. J.; Glinka, C. J.; Han, C. C. *Macromolecules* **1985**, *18*, 67.
- (16) Hashimoto, T.; Shibayama, M.; Kawai, H. *Macromolecules* **1983**, *16*, 1093.
- (17) Jinnai, H.; Hasegawa, H.; Hashimoto, T.; Han, C. C. *J. Chem. Phys.* **1993**, *99*, 4845, 8154.
- (18) Leibler, L. *Macromolecules* **1980**, *13*, 1602.
- (19) Shibayama, M.; Yang, H.; Stein, R. S.; Han, C. C. *Macromolecules* **1985**, *18*, 2179.

MA9613749